# Recent Results and Future Plans

**Generation of gauge configurations with the highly improved HISQ action**: Although our library of asqtad gauge ensembles is enabling the accurate determination of a wide range of physical quantities [1], there are a number of important calculations, particularly those related to tests of the standard model, that require greater accuracy than it can provide. For this reason, we have undertaken to generate a new library of gauge configurations using the Highly Improved Staggered Quark (HISQ) action developed by the HPQCD Collaboration [2]. Tests by HPQCD [2] and our own group [3] indicate that lattice spacing artifacts for the HISQ action are reduced by approximately a factor of 2.5 from those of the asqtad action for the same lattice spacing, and taste splittings in the pion masses are reduced sufficiently to enable us to undertake simulations with the Goldstone pion at or near the physical mass of the pion [3]. ("Taste" refers to the different ways one can construct the same physical particle in the staggered quark formalism. Although particles with different tastes become identical in the continuum limit, their masses can differ at finite lattice spacing). The reduction in taste splitting in going from the asqtad to HISQ configurations is shown in Fig. 1. In addition, the improvement in the quark dispersion relation enables us to include charm sea quarks in the simulations.

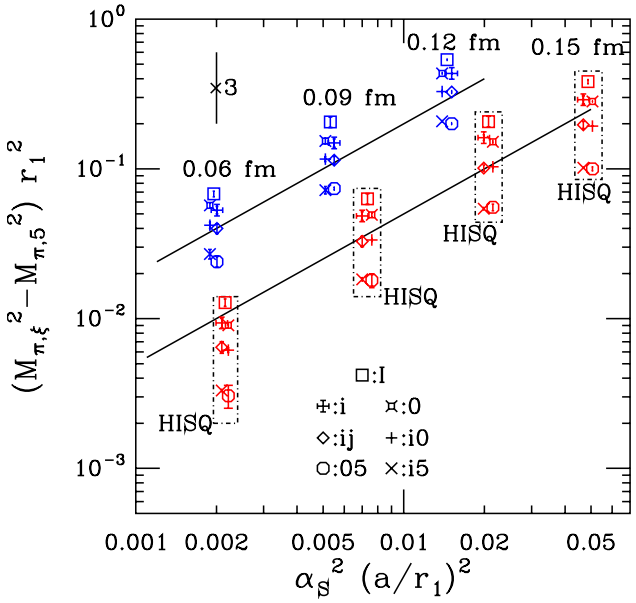


Figure 1: Taste splitting of pions for asqtad (blue) and HISQ (red) actions. For clarity, the HISQ splittings are also enclosed in dashed-dotted boxes, and nearly degenerate masses have been displaced slightly in the horizontal direction. Differences between the squared masses of various taste pions and that of the Goldstone pion are shown in units of the Sommer parameter $r_1$, and plotted versus the expected leading dependence of taste violations in the theory, $\alpha_S^2 a^2$, also in $r_1$ units. Here, we use $\alpha_S = \alpha_V$ at scale $q^* = 2/a$. The two diagonal lines are not fits, but merely lines with slope 1, showing the expectation if the splittings are linear in $\alpha_S^2 a^2$. The vertical line at the upper left shows the displacement associated with a factor of three in splittings.

We are generating HISQ gauge ensembles with four flavors of quarks: up, down, strange, and charm. For most ensembles, we tune the strange and charm quark masses, $m_s$ and $m_c$, to be as close as possible to their physical values and take the up and down quarks to be degenerate with a common mass $m_l$, which has an effect of less than 1% on isospin-averaged quantities. We are generating ensembles with three values of the light quark mass: $m_l/m_s = 1/5$, 1/10 and the value for

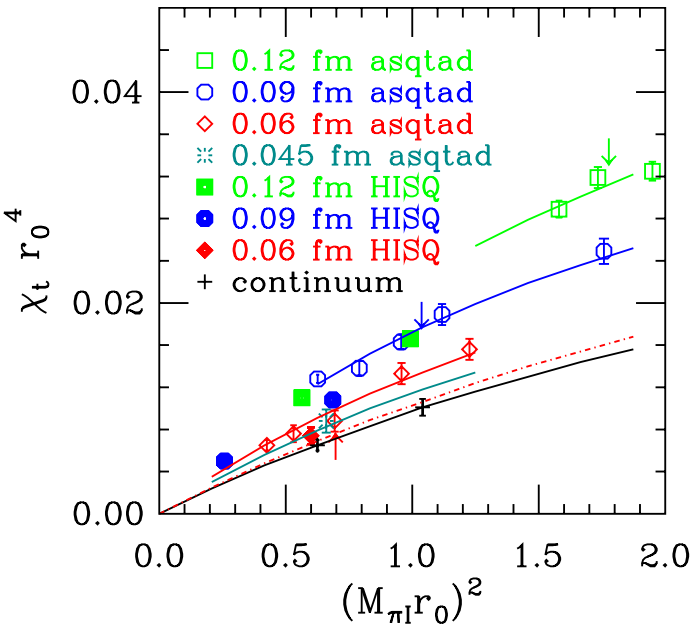


Figure 2: Topological susceptibility *vs.* taste-singlet pion mass squared in units of $r_0$, comparing results from five HISQ ensembles (filled symbols) with those from asqtad ensembles (open symbols). Solid curves are from a joint chiral/continuum fit to the asqtad data. The lowest (black) curve is the resulting continuum extrapolation of the asqtad fit with two representative points displaying the extrapolation errors. The (red) dot-dashed curve shows the leading order prediction in chiral perturbation theory. The (green) arrow above the (green) 0.12 fm asqtad curve indicates the asqtad point with a light quark mass comparable to that of the upper solid (green) HISQ square. Similarly, the (blue) arrow above the (blue) 0.09 fm asqtad curve indicates the asqtad point with a light quark mass comparable to the upper solid (blue) HISQ octagon, and the (red) arrow below the (red) 0.06 fm asqtad curve locates the asqtad point with a light quark mass comparable to the solid (red) HISQ diamond.

which the Goldstone pion mass is equal to the physical pion mass, which is approximately $m_l/m_s = 1/27$. These quark mass values correspond to Goldstone pion masses of 315 MeV, 222 MeV and 135 MeV, respectively. We have also generated a limited number of ensembles with the strange quark mass lighter than its physical value in order to aid in chiral extrapolations. The parameters of the ensembles we are generating in this project, and the number of equilibrated configurations we currently have in each ensemble, are shown in the link HISQ Lattice Generation. Detailed properties of the ensembles and the simulations which created them are given in Ref. [4]. We measure the static quark potential, the leptonic decay constants of $\pi$, $K$, $D$ and $D_s$ mesons, and the light and charm hadron spectra on these configurations as they are generated. In addition to being important in their own right, these measurements are needed to tune the lattice spacing and quark masses of the ensembles, and to monitor the progress of the runs. We determine the lattice spacing both by using the the $f_{p4s}$ scale [4, 5] and the gradient flow [6].

The topological susceptibility provides a particularly stringent test of the HISQ gauge configurations because it is computed from them without involving valence quarks. Thus, comparison of the topological susceptibility on the asqtad and HISQ configurations directly tests whether the change in sea quark action leads to the expected improvement in the gauge configurations. Figure 2 shows the topological susceptibility for most of the asqtad ensembles, as well as for HISQ ensembles with light quark mass $m_l = m_s/5$ and lattice spacings $a \approx 0.12$, 0.09 and 0.06 fm, and light quark mass $m_l \approx m_s/27$ and $a \approx 0.12$ and 0.09 fm. Note that the HISQ points with $a \approx 0.12$, 0.09 and 0.06 fm are near the asqtad curves with $a \approx 0.09$, 0.06 and 0.045 fm, respectively. The HISQ points are to

the left of the corresponding asqtad points because the horizontal axis is the mass of the taste singlet pion (the heaviest pion taste), and the reduction in taste symmetry breaking moves the HISQ points to the left. It is the decrease of the susceptibility for the HISQ configurations relative to those of the asqtad configurations that represents the improvement in the gauge configurations.

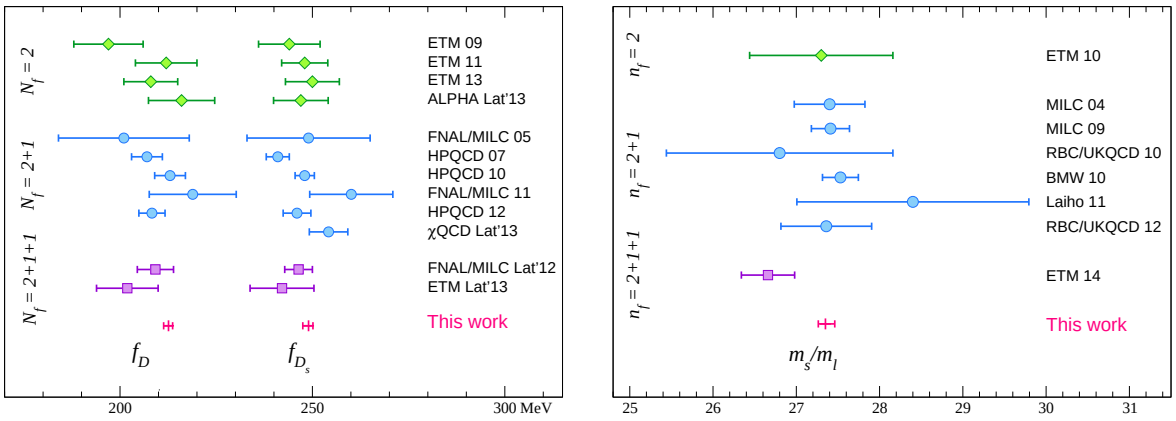


Figure 3: Comparison of our latest results for the leptonic decay constants $f_D$ and $f_{D_s}$ (left panel) and for the quark mass ratio $m_s/m_l$ (right panel) with earlier lattice calculations [8]. Results are grouped by the number of flavors of sea quarks from top to bottom: $N_f = 2$ (green diamonds), $N_f = 2+1$ (blue circles), and $N_f = 2+1+1$ (purple squares). Within each grouping, the results are in chronological order. Our new results are denoted by magenta pluses and labeled "This work".

**Light pseudoscalar mesons and quark masses**: The computation of properties of light pseudoscalar mesons offers a unique opportunity to check lattice methods to high precision and to calculate phenomenologically important physical quantities that are difficult or impossible to obtain with controlled errors by other methods. As noted above, we are measuring the masses and leptonic decay constants of $\pi$, $K$, $D^+$ and $D_s$ mesons, the heavy quark potential, and the light, strange and charm hadron spectra on the HISQ configurations as we generate them. Our first result from the physical quark mass HISQ ensembles came from a study of the leptonic decay constants of the $K$ and $\pi$ mesons [7]. In this work we determined $f_{K^+}/f_{\pi^+}$ to a precision of 0.4%, later improved to 0.2% with the addition of more configurations [8]. Combining this result with recent experimental data for the leptonic branching fractions, and the value of the CKM matrix element $|V_{ud}|$ determined from nuclear beta decay, enabled us to calculate the CKM matrix element $|V_{us}|$, and to check the unitarity of the first row of the CKM matrix at the $10^{-3}$ level.

With our colleagues in the Fermilab Lattice Collaboration we also used data from the pseudoscalar measurement code to calculate the leptonic decay constants of the $D^+$ and $D_s$ mesons, $f_{D^+}$ and $f_{D_s}$, and to determine ratios of a number of quark masses. Some of the key results are:

$$\begin{aligned} f_K/f_\pi &= 1.1957 \pm 0.0027 \\ f_{D^+} &= 212.3\,^{+1.0}_{-1.2}\ \text{MeV} \\ f_{D_s} &= 248.7\,^{+1.0}_{-1.5}\ \text{MeV} \\ m_c/m_s &= 11.74 \pm 0.06 \\ m_s/m_l &= 27.37 \pm 0.12 \end{aligned}$$

In Fig. 3 we compare some of these results to previous lattice calculations.

It is also possible to determine $|V_{us}|$ by calculating the vector form factor at zero recoil for the semileptonic decay $K \to \pi\ell\nu$. We and our Fermilab colleagues have used our HISQ gauge configurations for this purpose [9]. The current status of this calculation is shown in Fig. 4.

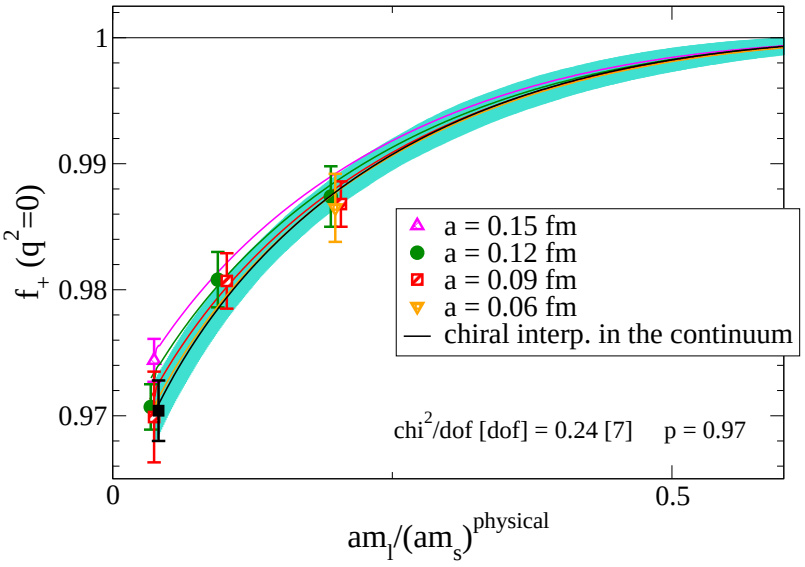


Figure 4: The form factor at zero recoil $f_+(0)$ as a function of the light-quark mass. Different symbols and colors denote different lattice spacings, and the corresponding colored lines show the chiral interpolation at fixed lattice spacing. The solid black line is the interpolation in the light-quark mass, keeping $m_s$ equal to its physical value, and turning off all discretization effects. The turquoise error band includes statistical, discretization, and higher order chiral errors.

We and our Fermilab colleagues are in the process of extending our work on leptonic decay constants to $B$ and $B_s$ mesons. The major improvements we obtained for the decay constants of the $D$ and $D_s$ mesons was made possible by the use of the HISQ action for charm-quarks; however, we can make use of the HISQ action to describe $b$-quarks on the lattice only for $am_b < 0.9$ if we are not to encounter large finite lattice spacing artifacts. The $a \approx 0.042$ and 0.03 fm ensembles meet this requirement, and will therefore play an important role in the analysis. For larger lattice spacings, we follow the suggestion of the HPQCD Collaboration [10] to perform calculations with a range of heavy-quark masses lighter than the $b$-mass, and extrapolate to the physics point. Very promising preliminary results were presented at Lattice 2015, and are illustrated in Fig. 5.

**Weak decays of particles containing heavy quarks**: At SLAC, KEK and Fermilab, a concerted experimental effort has been made to determine elements of the Cabibbo-Kobayashi-Maskawa (CKM) matrix through studies of the mixings and decays of B mesons. In addition, the properties of D mesons have been measured to high accuracy in the CLEO-c Program at Cornell. Work in this area continues in the LHCb and BES experiments. One hopes that by tightly over–constraining the CKM matrix elements, the range of validity of the standard model will be determined, and new physics beyond it will be discovered. However, the experimental results do not, in general, determine the CKM parameters without lattice calculations of the effects of the strong interactions.

Our group and the Fermilab Lattice Collaboration are involved in an extensive joint study of the decays of pseudoscalar mesons with one light and one heavy quark. The main subjects of our work are $B$, $B_s$, $D$, and $D_s$ mesons. We are studying both leptonic and semileptonic decays and the mixing between the neutral $B$ and $B_s$ mesons and their antiparticles. Strong interaction effects

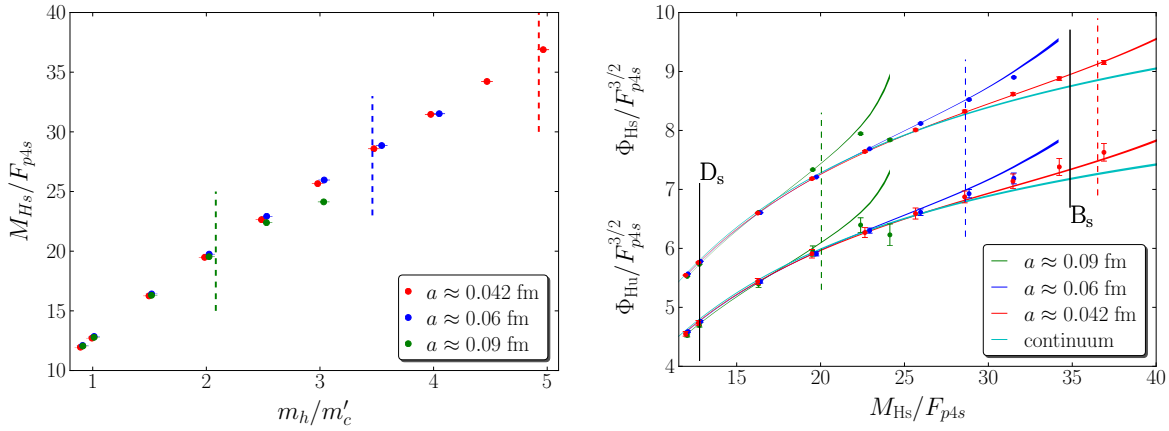


Figure 5: Illustration of heavy-quark discretization effects. Left panel: heavy-strange meson mass in units of $F_{p4s}$, which is approximately 154 MeV, versus the ratio of the heavy-quark mass to the simulation charm quark mass $m_h/m'_c$ for three lattice spacings at physical sea-quark masses. The small differences in the heavy-strange mass for different lattice spacings gives an indication of the heavy-quark discretization error. Right panel: the quantity $\Phi_{Hq} = f_{H_q}\sqrt{M_{Hq}}$, where $f_{Hq}$ is the leptonic decay constant and $M_{Hq}$ the mass the heavy-light meson, plotted in units of $F_{p4s}$ versus the heavy-strange meson mass $M_{Hs}$ for three lattice spacings and the continuum extrapolation. In both panels the dashed vertical lines indicate the cut $am_h = 0.9$ for each lattice spacing. Finite lattice spacing effects in the decay constant increase dramatically for large $am_h$, so we drop data with $am_h > 0.9$, and parameterize the heavy-quark mass dependence in our fits at smaller values with the help of heavy-quark effective theory.

in leptonic decays are characterized by the decay constants $f_B$, $f_{B_s}$, $f_D$, and $f_{D_s}$. Semileptonic decays are characterized by various form factors $f(q^2)$, where $q$ is the momentum transferred to the leptons, and the mixing of neutral $B$ and $B_s$ mesons with their antiparticles by bag parameters $B_B$ and $B_{Bs}$. CLEO-c provided precise measurements of the $D$ and $D_s$ leptonic and semileptonic decays. Comparisons of lattice and experimental results have provided an opportunity to validate our approach, and insure that we do, in fact, have full control over systematic errors. The successful predictions of the leptonic decay constants $f_D$ and $f_{D_s}$ [11] and the shape and normalization of the semileptonic form factors for $D$ mesons [12] by us and our Fermilab collaborators were important steps in this process. Since these initial calculations, steady progress has been made.

We have completed a study of mixing of neutral $B$ and $B_s$ mesons with their antiparticles using our asqtad ensembles with Fermilab heavy valence quarks [13, 14]. In this work have determined the SU(3)-breaking ratio, which measures the difference between the mixing parameters in the $B_s^0$ and $B_d^0$ systems, $\xi \equiv f_{B_s}\sqrt{B_{B_s}}/f_{B_d}\sqrt{B_{B_d}}$ to approximately 1.5%, the most precise measurement to date. Our determinations of the CKM matrix elements $|V_{td}|$ and $V_{ts}|$ from this calculation differ from CKM-unitarity expectations by up to $3\sigma$. These results and others from flavor-changing-neutral currents point towards an emerging tension between weak processes that are mediated at the loop and tree levels.

The BaBar Collaboration recently performed the first measurement of the exclusive semi-leptonic decay $B \to D\tau^-\bar{\nu}$, finding $R(D) \equiv \mathrm{BR}(B \to D\tau\nu)/\mathrm{BR}(B \to D\ell\nu) = 0.440(58)(42)$ [15], which is about two standard deviations away from previous theoretical expectations. This quantity is sensitive to beyond-the-standard-model physics, so it is important to solidify the theoretical calculations. Using lattice matrix elements already computed by us for other projects, we were able to evaluate the combination of form factors relevant to this decay, resulting in the first calculation in full QCD of the branching ratio $R(D)$ [16]. We found $R(D) = 0.316(12)(7)$, where the errors are statistical and total systematic, respectively. This result has recently been updated to $R(D) = 0.299(11)$ in the

course of our study of the reaction $\bar{B} \to D\ell\bar{\nu}$ [17], which is $2\sigma$ below the BaBar measurement [15]

We and our Fermilab collaborators have also calculated the SU(3) violating ratio of form factors for the semileptonic decays $\bar{B}^0 \to D^+\ell^-\bar{\nu}$ and $\bar{B}_s^0 \to D_s^+\ell^-\bar{\nu}$ [18]. This ratio, in combination with experimentally measured branching fractions for semileptonic and non-leptonic $B$ decays, can determine the ratio of fragmentation functions $f_s/f_d$ [19], which in turn allows experimental measurement of the rate for the decay $B_s^0 \to \mu^+\mu^-$. The latter decay is very interesting phenomenologically because it occurs only at the loop level in the standard model and, therefore is a sensitive probe of physics beyond the standard model. We find: $f_0^{(s)}(M_\pi^2)/f_0^{(d)}(M_K^2) = 1.046(44)_{\rm stat}(15)_{\rm syst}$. The ratio is consistent with $(d \leftrightarrow s)$ symmetry in contrast to an earlier estimate from QCD sum-rules [20]. Our result should significantly increase the sensitivity of the $B_s^0 \to \mu^+\mu^-$ measurements.

We and our Fermilab collaborators have recently completed a calculation of the zero-recoil form factor for the semileptonic decay $\bar{B}^0 \to D^{*+}\ell^-\bar{\nu}$ [21]. Our result leads to a determination of the CKM matrix element $|V_{cb}|$ in which the QCD error is now commensurate with the experimental error. We have also recently calculated the form factors for the decays $\bar{B} \to D\ell\bar{\nu}$ [17], $\bar{B} \to \pi\ell\nu$ [22], $B \to \pi\ell\ell$ [23], and $B \to K\ell\ell$ [24]. All of this work was performed on asqtad gauge configurations, and we are in the process of extending it to HISQ configurations which we expect to yield considerably more precise results.

**Electromagnetic contributions to the up and down quark masses**: The fundamental parameters of QCD are the strong coupling constant $\alpha_S$, and the masses of the quarks. The values of $\alpha_S$, and of the charm and bottom quark masses, $m_c$ and $m_b$ have been determined both from lattice calculations in the strong coupling regime, and from perturbative calculations in the weak coupling regime. (In both cases experimental data is coupled with theoretical calculations to obtain the final results). The lattice and perturbative calculations agree, and are of similar precision. On the other hand, the masses of the three lightest quarks, the up, down and strange, $m_u$, $m_d$, and $m_s$ respectively, can be obtained with controlled errors only from lattice calculations. We have recently obtained the mass ratios $m_s/m_l$ and $m_c/m_s$ to a precision of better than one-half a percent. Here the light quark mass $m_l = (m_u + m_d)/2$. These results, coupled with the high accuracy determination of $m_c$, enable one to obtain $m_s$ and $m_l$.

We are currently working on a calculation of the mass ratio $m_u/m_d$. A precise determination of this ratio, coupled with our current knowledge of $m_l$ will yield high precision results for $m_u$ and $m_d$ individually, completing the program of calculating the quark masses on the lattice.

Our QCD calculations yield very precise values of $m_u$, $m_d$, and $m_s$ in a fictitious world without electromagnetic interactions. To obtain the latter from real world data, one must determine the electromagnetic contributions to the masses of the the $\pi$ and $K$ mesons. The largest error in our current evaluation of $m_u/m_d$ comes from uncertainties in the size of these electromagnetic contributions, especially for the $K$ mesons. These effects also give significant errors to other quark mass ratios and to the quark masses themselves. Until recently, the electromagnetic contributions had to be taken from continuum phenomenology. A conservative interpretation of the errors in the continuum calculations results in a 20% error for $m_u/m_d$, and even a rather aggressive interpretation leaves a 10% error [25]. However, this problem can be addressed directly on the lattice by including electromagnetic effects in the simulations.

A first step is to treat the electromagnetic field in the quenched approximation. In this approximation, photons only couple to the explicit "valence" quarks inside a hadron, and do not couple to virtual quark-antiquark pairs. In other words, the quarks in virtual quark-antiquark pairs are taken to be electromagnetically uncharged. Fortunately, it turns out [26] that, through next-to-leading order (NLO) in chiral perturbation theory, the meson mass differences relevant to $m_u/m_d$ can be computed using a quenched electromagnetic field without the uncontrolled systematic errors usually associated with quenching. This fact enables us to use our existing QCD gauge configurations, and to independently generate electromagnetic field configurations neglecting the back reaction of

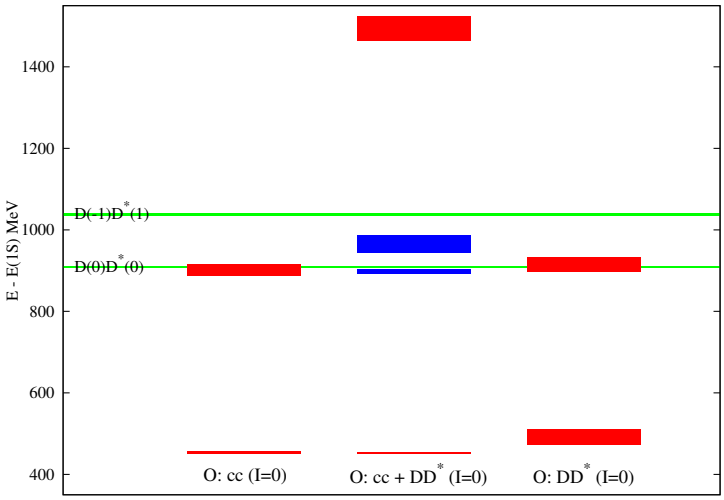


Figure 6: Energy levels from the variational calculation of the $X(3872)$. The horizontal green lines locate the non-interacting $D(0)D^*(0)$ and $D(-1)D^*(1)$ levels (at the two lowest discrete momenta). Left column contains the unmixed $\chi_{c1}(1P)$ and $\chi_{c1}(2P)$ states. The middle column has shows the mixed $cc$ and $DD^*$ states resulting in the $X(3872)$ and a $DD^*$ scattering states. The right column contains the unmixed $D(0)D^*(0)$ and $D(-1)D^*(1)$ states. The lower blue bar represents the $X(3872)$ with a binding energy relative to the $D\bar{D}^*$ threshold of $13(6)$ MeV with our unphysical lattice parameters.

sea quarks.

We are in the process of completing a computation with quenched QED and the asqtad QCD ensembles with lattice spacings ranging from 0.15 fm to 0.045 fm, and light quark masses down to 1/20 of the strange quark mass [27, 28, 29, 30]. The goal of the computation is a determination of the parameter $\varepsilon$, which relates the EM splitting of the kaons to that of the pions: $\Delta M_K^2 = (1+\varepsilon)\Delta M_\pi^2$. Our preliminary result is $\varepsilon = 0.73(14)$, which results in an uncertainty in $m_u/m_d$ due to electromagnetic effects of about 2.5%. Although this is a gratifying reduction from the 10% error obtained with phenomenological estimates, electromagnetic effects remain the dominant error, by a wide margin, in our determination of $m_u/m_d$. We therefore plan to extend this calculation to the HISQ gauge configurations.

We expect use of the HISQ configurations to provide a major reduction in errors because of their smaller discretion effects, their nearly vanishing chiral extrapolation errors, the use of ensembles with physical quarks masses, and smaller finite-volume effects.

**Quarkonium**: Heavy quarks and antiquarks (charm and bottom) form bound states analogous to positronium — hence the name "quarkonium". Since their discovery in the 1970's, many dozens of states of charmonium and bottomonium have been studied experimentally. Below the open charm or open bottom threshold energy — the threshold for decay into pairs of mesons consisting of a heavy quark and light antiquark, the states have small measured widths, and provide exacting tests of our theoretical ability to make high precision predictions of the properties of states involving heavy quarks. Higher states are found, but their interpretation in quark-model language is uncertain. Some may be "hybrid exotics", states that include a valence gluon in addition to a valence quark and antiquark. Their existence has yet to be confirmed. Lattice QCD is the only *ab initio* tool for guiding the classification of these and other mysterious states.

We are completing a major study of charmonium using Fermilab quarks [32]. Analysis of the final results is still underway; however, it is already clear that our use of improved stochastic sources and a larger set of interpolating operators is providing a much cleaner spectrum than we had obtained in earlier work. We plan to extend our study to bottomonium working with the new set of HISQ gauge configurations. As we have demonstrated with charmonium, we expect that we will greatly improve statistical accuracy compared with our previous study [33]. There are three sources of improvement: (1) For the first time we will include calculations at physical values of all the sea quark masses, thus reducing errors coming from the chiral extrapolation. (2) Our interpolating operators will be constructed from random sources, thus making full use of the lattice volume. (3) Our lattice volumes are larger than before, effectively increasing the statistical sample size.

We are also in the process of carrying out a study of the $X(3872)$ meson. The $X(3872)$ is a well-established charmonium state that cannot be explained in the conventional quark model. Since it appears very close to the $D\bar{D}^* - \bar{D}D^*$ meson threshold (very weakly bound), it has been suggested that it is a tetraquark or a molecular state consisting of charm and anticharm quarks plus a light quark-antiquark pair. Lattice QCD is the only *ab initio* method for testing whether QCD can explain the existence of this state and provide insights into its nature. To succeed, it is necessary to use an interpolating operator basis that includes operators that generate a charm quark/antiquark pair ($\bar{c}c$) as well as operators that contain explicit $D$ and $D^*$ mesons ($DD^*$). In the first phase of this work we used the HISQ ensemble with $a \approx 0.15$ fm and $m_l = m_s/5$ to confirm the result of the Slovenia group [34] that mixing between the $\bar{c}c$ and $DD^*$ channels can yield a state with the properties of the $X(3872)$, as is shown in Fig. 6. In the second phase of our study we are using an ensemble with the same lattice spacing and physical sea quark masses to investigate whether this state survives in a more realistic calculation.

We are also undertaking an exploratory study of charmonium using the HISQ formalism for the charm valence quarks, which promises even higher precision in determining charmonium levels. This study will be the first of its kind to use a large variational basis set. We have also begun an exploratory charmonium study including a $D\bar{D}^*$ open charm interpolating operator to see if it improves the calculation.

## References


[1] The MILC Collaboration: A. Bazavov *et al.*, Rev. Mod. Phys. **82**, 1349-1417 (2010) [arXiv:0903.3598 [hep-lat]].

[2] The HPQCD/UKQCD Collaboration: E. Follana, *et al.*, Nucl. Phys. B (Proc. Suppl.) **129** and **130**, 447 (2004); Nucl. Phys. B (Proc. Suppl.) **129** and **130**, 384 (2004); Phys. Rev. **D75**, 054502 (2007).

[3] The MILC Collaboration: A. Bazavov *et al.*, Phys. Rev. D **82**, 074501 (2010) [arXiv:1004.0342].

[4] The MILC Collaboration: A. Bazavov *et al.*, Phys. Rev. **D87**, 054505 (2013) [arXiv:1212.4768].

[5] The HPQCD Collaboration: C.T.H. Davies *et al.*, Phys. Rev. D **81**, 034506 (2010), [arXiv:0910.1229].

[6] The MILC Collaboration: A. Bazavov *et al.*, Proceedings of Science (Lattice 2013) 269 (2013) [arXiv:1311.1474]; Proceedings of Science (Lattice 2014) 090 (2014) [arXiv:1411.0068]; arXiv:1503.02769, submitted to Phys. Rev. D.

[7] The MILC Collaboration: A. Bazavov *et al.*, Phys. Rev. Lett. **110**, 172003 (2013) [arXiv:1301.5855].

[8] The Fermilab Lattice and MILC Collaborations: A. Bazavov *et al.*, Proceedings of Science (Lattice 2013) 405 (2013) [arXiv:1312.0149]. Phys. Rev. D**90**, 074509 (2014) [arXiv:1407.3772].

[9] The Fermilab Lattice and MILC Collaborations: A. Bazavov, *et al.*, Phys. Rev. Lett. **112**, 112001 (2014) [arXiv:1312.1228].

[10] The HPQCD Collaboration: C. McNeile, *et al.*, Phys. Rev. **D85**, 031503 (2012) [arXiv:1110.4510]; Phys. Rev. **D86**, 074503 (2012) [arXiv:1207.0994].

[11] The Fermilab Lattice, MILC and HPQCD/UKQCD Collaborations: C. Aubin *et al.*, Phys. Rev. Lett.**95**, 122002 (2005).

[12] The Fermilab Lattice, MILC, and HPQCD/UKQCD Collaborations: C. Aubin *et al.*, Phys. Rev. Lett. **94**, 011601 (2005) [arXiv:hep-lat/0408306].

[13] The Fermilab Lattice and MILC Collaborations: A. Bazavov, *et al.*, Phys. Rev. **D86**, 034503 (2012) [arXiv:1205.7013].

[14] The Fermilab Lattice and MILC Collaborations: A. Bazavov, *et al.*, arXiv:1602.03560.

[15] J.P. Lees *et al.*, (BaBar Collaboration) (2012), arXiv:1205.5442 [hep-ex].

[16] The Fermilab Lattice and MILC Collaborations: J. A. Bailey, *et al.*, Phys. Rev. Lett. **109**, 071802 (2012) [arXiv:1206.4992].

[17] The Fermilab Lattice and MILC Collaborations: Jon A. Bailey, *et al.*, Phys.Rev. D92 (2015) 3, 034506 [arXiv:1503.07237].

[18] The Fermilab Lattice and MILC Collaborations, J. A. Bailey, *et al.*, Phys. Rev. D **85**, 114502 (2012) [arXiv:1202.6346].

[19] R. Fleischer, N. Serra and N. Tuning, Phys. Rev. D **82**, 034038 (2010) [arXiv:1004.3982]; R. Aaij *et al.* [LHCb Collaboration], Phys. Rev. Lett. **107**, 211801 (2011) [arXiv:1106.4435].

[20] P. Blasi, P. Colangelo, G. Nardulli and N. Paver, Phys. Rev. D **49**, 238 (1994) [hep-ph/9307290].

[21] The Fermilab Lattice and MILC Collaborations: J.A. Bailey, *et al.*, Phys. Rev. D**89**, 114504 (2014) arXiv:1403.0635.

[22] The Fermilab Lattice and MILC Collaborations: Jon A. Bailey, *et al.*, Phys. Rev. D**92**, 014024 (2015) [arXiv:1503.07839].

[23] The Fermilab Lattice and MILC Collaborations, J. Bailey, *et al.*, Phys. Rev. Lett. **115**, 152002 (2015) [arXiv:1507.01618].

[24] The Fermilab Lattice and MILC Collaborations: J. Bailey, *et al.*, arXiv:1509.06235. To appear in Phys. Rev. D.

[25] The MILC Collaboration: C. Aubin *et al.*, Phys. Rev. D**70**, 114501 (2004); Nucl. Phys. B (Proc. Suppl.) **140**, 231 (2005); Proceedings of Science (Lattice 2005) 025 (2005); Proceedings of Science (Lattice 2006) 163 (2006); Proceedings of Science (Lattice 2007) 090 (2007); Proceedings of Science (Chiral Dynamics) CD09 (2009); Proceedings of Science (Lattice 2010) 074 (2011).

[26] J. Bijnens and N. Danielsson, Phys. Rev. D **75**, 014505 (2007) [arXiv:hep-lat/0610127].

[27] The MILC Collaboration: S. Basak *et al.*, Proceedings of Science (Lattice 2008), 127 (2008) [arXiv:0812.4486 [hep-lat]].

[28] The MILC Collaboration: S. Basak *et al.* Proceedings of Science (Lattice 2012) 137 (2012) [arXiv:1210.8157]; Contribution to the 7th International Workshop on Chiral Dynamics, Jefferson Laboratory, Newport News, VA, August, 2012 [arXiv:1301.7137].

[29] The MILC Collaboration: S. Basak *et al.*, to be published in Proceedings of Science (LATTICE 2014), 116 (2014).

[30] The MILC Collaboration: S. Basak *et al.*, Proceedings of the XXVI IUPAP Conference on Computational Physics (CCP2014), Phys. Conf. Ser. 640 012052 [arXiv:1510.04997].

[31] C. DeTar *et al.* [Fermilab Lattice and MILC Collaboration], PoS **LATTICE2012**, 257 (2012) [arXiv:1211.2253]; D. Mohler, *et al.*, PoS **LATTICE2014** (2014) [arXiv:1412.1057].

[32] T. Burch *et al.*, Phys. Rev. D **81** 034508 (2010) [arXiv:0912.2701 [hep-lat]].

[33] S. Prelovsek and L. Leskovec, Phys. Rev. Lett. **111**, 192001 (2013) [arXiv:1307.5172 [hep-lat]].